Aalborg University

DENMARK

Cyber Physical Energy Systems Modules for Power Sharing Controllers in Inverter Based Microgrids

Macana, Carlos A.; Abdou, Ahmed F.; Pota, Hemanshu R.; Guerrero, Josep M.; Vasquez, Juan C.

Article

Cyber Physical Energy Systems Modules for Power Sharing Controllers in Inverter Based Microgrids

Carlos A. Macana [1,*] (ID) **, Ahmed F. Abdou** [1] (ID) **, Hemanshu R. Pota** [1] (ID) **, Josep M. Guerrero** [2] (ID) **and Juan C. Vasquez** [2] (ID)

[1] School of Engineering and Information Technology, University of New South Wales, Canberra 2612, Australia; a.abdou@adfa.edu.au (A.F.A.); h.pota@adfa.edu.au (H.R.P.)

[2] Institute of Energy Technology, Aalborg University, 9100 Aalborg, Denmark; joz@et.aau.dk (J.M.G.); juq@et.aau.dk (J.C.V.)

* Correspondence: carlos.macana@student.adfa.edu.au; Tel.: +61-2-6268-8197

Abstract: The Microgrids (MGs) are an effective way to deal with the smart grid challenges, including service continuity in the event of a grid interruption, and renewable energy integration. The MGs are compounded by multiple distributed generators (DGs), and the main control goals are load demand sharing and voltage and frequency stability. Important research has been reported to cope with the implementation challenges of the MGs including the power sharing control problem, where the use of cybernetic components such as virtual components, and communication systems is a 'common characteristic. The use of these cybernetic components to control complex physical systems generates new modeling challenges in order to achieve an adequate balance between complexity and accuracy in the MG model. The standardization problem of the cyber-physical MG models is addressed in this work, using a cyber-physical energy systems (CPES) modeling methodology to build integrated modules, and define the communication architectures that each power sharing control strategy requires in an AC-MG. Based on these modules, the control designer can identify the signals and components that eventually require a time delay analysis, communication requirements evaluation, and cyber-attacks' prevention strategies. Similarly, the modules of each strategy allow for analyzing the potential advantages and drawbacks of each power sharing control technique from a cyber physical perspective.

Keywords: microgrids; power electronics; power sharing control; cyber-physical energy systems; communications

1. Introduction

A low voltage power grid with distributed generation and the functionality to operate autonomously or connected to the main grid is known as Microgrid (MG) [1]. MGs have been visualized as an efficient structure for the conventional power systems restrictions, and an effective way to deal with the main challenges in a smart grid including load control, self-healing, and reliability under the new environmental constraints [2]. MGs have helped to increase the penetration of alternative energy sources such as Photovoltaic systems (PV), wind generation, fuel cells, biomass and batteries with storage facilities in power generation portfolios, which contribute to reducing environmental pollution from conventional energy resources. Although the MGs are likely to be a interesting solution to most of the important challenges of the conventional power systems, and the power electronic based technology in microgrids can offer better quality of power supply, greater dependability of service, and higher efficiency of energy [3], these benefits imply dealing with new

implementation and operation problems resulting from the integration of inverter-based distributed generators (IDGs), which requires of DC–AC inverter interfaces [4].

The main tasks of the MG controller are to ensure disconnection and reconnection processes, guarantee that the energy sources work accurately at the predefined operating point (or slightly different but still satisfy the operating limits), supply sensitive loads uninterruptedly, and operate with an adequate power sharing performance [5,6]. The control strategies for active power sharing have shown good results using a conventional droop controller and inductive line impedance; however, the reactive power sharing seems to be an open challenge [7]. Communication-based techniques such as concentrated control [8] and master/slave control [9] were the initial proposals to address the MG power sharing problem. These early approaches can achieve high-power quality, fast transient response, and tight current sharing, reducing the circulating currents between the inverter based generators, and have showed good performance in terms of voltage regulation. However, the high dependency on communications infrastructure and high bandwidth requirements imply lower reliability and extendability, and higher implementation cost [6]. These drawbacks have been reduced using decentralized techniques (also known as local information based-control techniques [10]). These strategies operate without inter-unit communications, and the most used techniques are the conventional droop controllers [11], the hybrid droop/signal injection method [12], impedance output loop techniques [13], virtual frame transformation [14], construct and compensate based methods [15,16] and these variants [17–19]. The droop controller is the most common technique owing to its plug-and-play characteristic, which allows the connection and disconnection of generation units without turning off the whole system. However, this control approach implies some potential drawbacks including voltage and frequency deviation from the desired values, slow transient response, and line parameter dependency [20].

On the other hand, several research works have claimed that the characteristics of the smart grids require new modeling methodologies, which can integrate cybernetic and physical layers of the system and offer an adequate balance between complexity and accuracy [21,22]. In this scenario, the cyber-physical modeling methodologies have emerged as an interesting tool to model and control the new smart grids, including the intelligent microgrids [23]. Recent works have addressed problems related with cybernetic requirements or constraints including cyber-attacks and operational reliability [23,24], time delay impact [25–28], and optimal operation using communication infrastructure and cooperative control approaches [29,30]. However, according to the best knowledge of the authors, a Cyber-Physical integrated modeling methodology for AC Microgrids applications requires further research owing to the lack of standardization of the the different control strategies and the modeling methodologies.

This work addresses the standardization problem of the Cyber-Physical characteristics of an AC-MG, and proposes a modular modeling methodology to analyze secondary control level and the new trends in power sharing controllers. This approach is useful to describe the main cybernetic and physical components of the new power sharing control strategies, including communications and virtual elements in the cybernetic layer, and physical electric circuits and components in the physical layer. The cyber-physical energy system (CPES) modeling methodology used in this work is based on the proposal for conventional power systems presented in [31], and develops CPES modules for IDGs with different power sharing control strategies. As a result of the CPES modeling methodology, a clear identification of internal and external cybernetic and physical signals of each studied controller is achieved. Additionally, the obtained model offers adequate flexibility to perform reliability and stability analysis considering both cybernetic and physical layers. Note that this paper is an extended version of the conference paper [10], but the following new substantial contributions are made:

- The power sharing problem for inverter based MGs is presented in detail in a CPES context.
- New trends to solve the open challenges on MG power sharing are presented and classified.
- The main communication architectures that are typically used in the new power sharing control strategies are identified and classified.

- A CPES methodology is used to obtain standard modules for each strategy and identify the main cybernetic and physical characteristics.
- New power sharing CPES modules have been developed including the Cooperative-Adaptive Synchronous Reference Frame (SRF) Virtual Impedance strategy module.

This paper is organized as follows: first, the power sharing problem for AC-MGs is discussed in Section 2. Second, the CPES modeling approach is presented in Section 3. In Section 4, different new trends of power sharing control strategies are modeled based on the CPES modeling methodology, obtaining a CPES module for each control strategy. Finally, a comparison of the different CPES characteristics of each strategy is presented in Section 5 and some conclusions are given in Section 6.

Preliminaries and Notation

The set of real, and nonnegative real numbers are detonated as $\mathbb{R}$, and $\mathbb{R}_{\geq 0}$, respectively. In a similar way, $\mathbb{N}$ denotes the set of natural numbers, $\mathbb{C}$ the set of complex numbers, and $\mathbb{S} := [0, 2\pi)$. Bold style denotes column vectors (e.g., $\mathbf{x}$), and scalars are notated by non-bold style (e.g., a). Matrices are denoted with capital letters and non-style (e.g., A). The set of IDGs in the AC-MG is denoted as $\mathcal{N} = \{1, \ldots, n\}$, where $n \in \mathbb{R}_{\geq 0}$, and $C_i \subseteq \mathcal{N}$ denotes the set of neighbors of the ith IDG, where $k \in C_i$ if the IDG_i and IDG_k can exchange their local measurements with each other. Let $\mathbf{x} = \mathrm{col}(x_1, \ldots, x_n) \in C_i$ denote a column vector with entries $x_i \in C_i$. To simplify the notation , we write $\mathbf{x} = \mathrm{col}(x_i) \in C_i$. For $a \in \mathbb{C}$, $|a|$ is the magnitude of a. A three phase symmetric signal $\mathbf{x}_{abc} : \mathbb{R}_{\geq 0} \to \mathbb{R}^3$ can be described by: let us consider a three-phase symmetric signal $\mathbf{x}_{abc} : \mathbb{R}_{\geq 0} \to \mathbb{R}^3$, which can be described by:

$$\mathbf{x}_{abc} = a(t) \begin{bmatrix} \sin(\delta_i) \\ \sin(\delta_i - 120°) \\ \sin(\delta_i + 120°) \end{bmatrix},$$

where the phase angle $\delta_i : \mathbb{R}_{\geq 0} \to \mathbb{S}$, and the amplitude $a(t) : \mathbb{R}_{\geq 0} \to \mathbb{R}_{\geq 0}$ describe completely the signal. Additionally, from the "Reference Frame Theory", the following transformations are defined as [32]:

$$\mathbf{x}_{\alpha\beta} = \begin{bmatrix} x_\alpha \\ x_\beta \end{bmatrix} = T_{abc \to \alpha\beta} \mathbf{x}_{abc},$$

where it is known as the "Clarke's Transformation", and

$$T_{abc \to \alpha\beta} = \frac{2}{3} \begin{bmatrix} 1 & -\frac{1}{2} & -\frac{1}{2} \\ 0 & \frac{\sqrt{3}}{2} & -\frac{\sqrt{3}}{2} \end{bmatrix}$$

and

$$\mathbf{x}_{dq} = \begin{bmatrix} x_d \\ x_q \end{bmatrix} = T_{\alpha\beta \to dq}(\hat{\delta}_i) \mathbf{x}_{\alpha\beta},$$

where it is known as the "Park's Transformation", and

$$T_{\alpha\beta \to dq}(\hat{\delta}_i) = \begin{bmatrix} \cos(\hat{\delta}_i) & \sin(\hat{\delta}_i) \\ -\sin(\hat{\delta}_i) & \cos(\hat{\delta}_i) \end{bmatrix}$$

and $\hat{\delta}_i \in \mathbb{S}$.

2. Power Sharing Problem in Islanded Microgrids

As an operation requirement, the distributed generators of an islanded MG should share the total power demand according to their nominal capacities [14,33]. A simple MG architecture is shown in Figure 1, where it is composed by loads $(1, 2, \ldots, m)$ and IDGs $(1, 2, \ldots, n)$. The loads are

assumed as constant impedances, and the IDGs as voltage controlled sources. Fixing the references values of amplitude voltages, and angular frequencies in each IDG, the power sharing between IDGs typically is non-proportional to their nominal powers. In Figure 2, the transient response to a load change in the MG with two single-phase IDGs and equal power ratings is presented. Each generator changes its respective active and reactive power output (p_1, p_2, q_1 and q_2), and the dynamic response is stable; however, the IDG_1 operates in an overload condition after the change of load demand. Additionally, the instantaneous circulating current ($i_{a,1}$-$i_{a,2}$) is increased until amplitude levels of 50 A. This condition could be avoided if each IDG shares power proportionally to its nominal power capacities. The requirement of each IDG sharing its output power proportionally to its nominal power is summarized in the following definition.
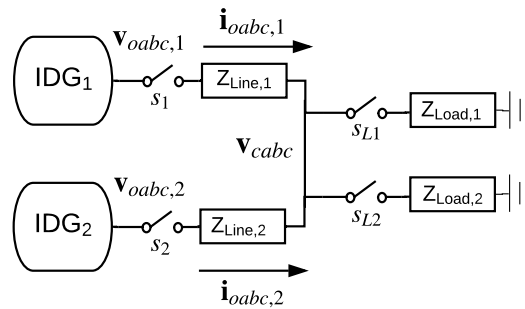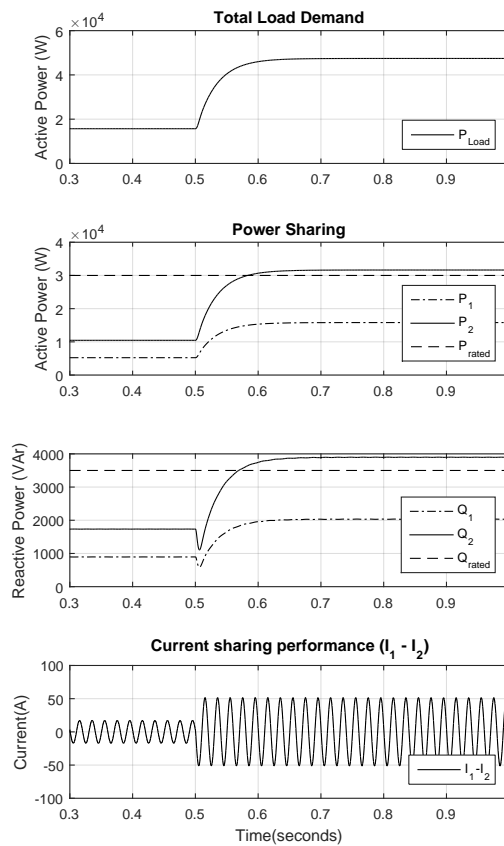

Figure 1. MG architecture.

Figure 2. Transient response to a load change in an MG without power sharing control.

Definition 1. *Considering p_i^{ss} and q_i^{ss} as the steady state active and reactive power outputs of the ith IDG, and for any given $\chi_i \in \mathbb{R}_{>0}$ and $\gamma_i \in \mathbb{R}_{>0}$ as weighting factors, a proportional power sharing is achieved between two IDGs at nodes i and k with $i \in \mathcal{N}$ and $k \in \mathcal{N}$ if [34]:*

$$\frac{p_i^{ss}}{\chi_i} = \frac{p_k^{ss}}{\chi_k}, \qquad \frac{q_i^{ss}}{\gamma_i} = \frac{q_k^{ss}}{\gamma_k}.$$

The parameters χ_i, γ_i, χ_k and γ_k can be selected as the per unit values of the active and reactive power ratings of each IDG.

The Conventional Droop Control

A common approach to tackle with the power sharing problem is the conventional droop control method [11]. This strategy uses the frequency and the amplitude voltage to control the active and reactive power injected by each IDG. To explain the droop control principle, a simplified IDG can be represented as a voltage controllable source (VSC) with controllable voltage magnitude and frequency (or phase) [35]. Figure 3 shows two VSC setting up a simple MG, operating in islanded mode.
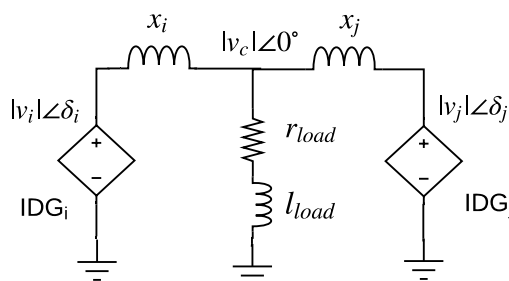

Figure 3. Equivalent circuit of the MG model.

Applying the conventional droop control method, the control variables (angular frequency and magnitude voltage) are defined as [11]:

$$\omega_i = \omega_n - m_i \cdot p_{m,i}, \tag{1}$$

$$v_i = v_n - n_i \cdot q_{m,i}, \tag{2}$$

where ω_i and v_i are the reference frequency and voltage magnitude, and $\omega_i = \dot{\delta}_i$. Additionally, ω_n and v_n, respectively, are the nominal angular frequency and voltage of the IDGs, n_i and m_i are the droop coefficients, and $p_{m,i}$ and $q_{m,i}$ are the measured active and reactive output powers from the *i*th IDG. The dynamics of the MG system depend in an important manner on the power measurement method [36], which is typically performed by a first order low pass filter described as [37–39]:

$$\tau_c \dot{p}_{m,i} = -p_{m,i} + p_i, \tag{3}$$

$$\tau_c \dot{q}_{m,i} = -q_{m,i} + q_i, \tag{4}$$

where $\tau_c \in \mathbb{R}_{\geq 0}$ is the time constant of the low pass pass filter, and p_i and q_i are the instantaneous power active and reactive values calculated as:

$$p_i = v_{\alpha,i} i_{\alpha,i} + v_{\beta,i} i_{\beta,i}, \tag{5}$$

$$p_i = v_{\beta,i} i_{\alpha,i} - v_{\alpha,i} i_{\beta,i}, \tag{6}$$

and $v_{\beta,i}$, $v_{\alpha,i}$, $i_{\alpha,i}$, and $i_{\beta,i}$ are the quarter-cycle delayed conjugated signal of the instantaneous voltage and current measurement signals, which can be obtained applying the Clarke's Transformation to

the measured instantaneous three-phase signals $\mathbf{v}_{abc,i}$, and $\mathbf{i}_{abc,i}$. As the voltage magnitude and the frequency must be regulated strictly, the values of droop constants are limited by $m = \frac{\Delta\omega}{p_{max}}$ and $n = \frac{\Delta e}{q_{max}}$ [39], where p_{max} and q_{max} are the maximum active and reactive power that can be delivered and Δw and Δe are the the maximum allowed frequency and magnitude voltage to avoid synchronization issues [14,37]. According to the equivalent circuit in Figure 3, the output apparent power (s_i) of the *i*th IDG is given by $s_i = p_i + jq_i$, where p_i and q_i are given by [40]:

$$p_i = \frac{|v_i||v_c|}{x_i}\sin(\delta_i), \tag{7}$$

$$q_i = \left[\frac{|v_i||v_c|\cos\delta_i - |v_c|^2}{x_i}\right]. \tag{8}$$

Considering the assumption $\delta_i \approx 0$, then $\sin(\delta_i) \approx \delta_i$, and we can obtain:

$$p_i = \frac{|v_i||v_c|}{x_i}\delta_i. \tag{9}$$

From the $\omega - P$ droop Equation (1), and differentiating from both sides of (9) yields

$$\dot{p}_i = \frac{|v_i||v_c|}{x_i}\dot{\delta}_i = \frac{|v_i||v_c|}{x_i}\omega_i = \frac{|v_i||v_c|}{x_i}(\omega_n - m_i \cdot p_{m,i}). \tag{10}$$

In steady state ($\dot{p}_i = 0$), the last equation leads to:

$$\frac{p_{m,i}}{m_i} = \frac{p_{m,j}}{m_j}, \tag{11}$$

and we can see that the steady state active power achieves the proportional power sharing introduced in Definition 1, if the frequency droop control parameters are tuned as: $m_i = \chi_i, \forall i \in N$. On the other hand, according to (2) and (8), the reactive power delivered by the i_{th} IDG could be obtained as [41]:

$$q_i = \frac{|v_c|(|v_n|cos(\delta_i) - |v_c|)}{x_i + |v_c|n_i\cos(\delta_i)}. \tag{12}$$

Additionally, assuming $\cos\delta_{ik} \approx 1$ as δ_{ik} is typically small, from (12), it can be obtained:

$$\Delta q = \frac{q_i - q_k}{q_i} = \frac{x_k - x_i}{x_k + |v_c|n_k}, \tag{13}$$

where Δq is the reactive power sharing error between the *i*th and the *j*th IDG. Thus, the conventional droop controller results in a finite reactive power sharing error (Δq). This error depends on the voltage droop parameter value (n_i), and the mismatch on the line impedance [41,42]. The reactive power sharing error might lead to another operation issues including overload power and over-voltage, which could affect the system reliability critically [43]. Some variations of the conventional droop control strategy have been proposed including the virtual impedance approach [37], which can achieve an important reduction of the reactive power sharing error but requires accurate feeder impedance estimation through online or offline methods. In this context, most of the recent power control strategies use different communication architectures to achieve accurate power sharing. In the next section, the CPES modeling methodology will be applied to AC-MG modeling.

3. Cyber Physical Microgrid Modeling

The CPES modeling methodology proposed in [31] is an interesting tool to characterize an MG with IDGs because it offers different advantages compared to the conventional modeling approaches, which could lead to neglecting essential cybernetic interactions and affecting the model accuracy

and the system's reliability. Stability issues owing to time delays in communications [44] are one of the most common cybernetic conditions that should be considered. This interaction between cybernetic and physical layers can be included in the design process like a CPES in order to guarantee the model accuracy and a reliable operation [22,45]. Using a CPES modeling methodology offers different advantages with respect to the classical modeling approaches. Firstly, this approach allows a flexible integration of the different components in an MG, which provides zooming-in and zooming-out capabilities to characterize specific system components and interactions between modules. Additionally, the methodology has been designed as a systematic method to integrate unconventional energy sources to the future energy systems; consequently, this approach leads to a modular representation of an IDG as a main component of an MG. This methodology can be followed in order to use the model obtained for analyzing the system-wide observability, and to evaluate integrally the performance in terms of stability and controllability [31]. Hence, CPES modeling methodologies are likely to be needed in order to achieve an integral approach to MG design. The CPES modeling approach includes two main steps [31]:

1. Build a CPES module for each component of the large scale system characterized by physical and cybernetic input and output signals as well as internal dynamics, local sensing and actuation.
2. Integrate CPES modules following network constraints.

This work performs the first step of the methodology, and different IDG-CPES modules are developed for the most recent power sharing control strategies for inverter based MGs. The development of the cybernetic and physical network models required for the second step of the CPES modeling methodology is the next stage of our research.

Interesting advances have been already performed from the physical [40] and cybernetic perspective [46]. However, according to the best knowledge of the author, an integrated CPES approach has not been found in the literature. The communication and power network model is necessary to integrate each CPES module following network constraints. The physical layer network (power network) can be represented by the scheme shown in Figure 1. The cybernetic network depends on the information requirements of each control strategy. These different control approaches can be classified in two main categories: communication-based strategies and local information-based strategies. Owing to the fact that most of the local information based strategies have not offered a complete solution for the accurate power sharing problem, different communication based approaches have been proposed to tackle these gaps in the literature [34,42,45,47].

3.1. Dynamic Models for the CPES Microgrid Modules

Different alternatives for modeling the physical process of an inverter based distributed generator have been proposed, which include detailed temporary models and reduced models [48–50]. Detailed temporary IDG models might lead to 15th and 36th order mathematical state space linearized models for basic cases of two nodes in grid-tied, and islanded modes [48,49]. For this reason, reduced models have been proposed recently, but they are likely to offer a high grade of complexity too [40,48–50]. As an alternative, dynamic phasors-based modeling has been recently proposed [50]. This approach offers an accurate dynamic model with a tolerable level of complexity, which is important to achieve a proper flexibility and capability of zooming out to capture the dynamic interactions between CPES modules [31]. However, a characterization of cybernetic components such as communication topologies and a model structure that allows an integration with networked constraints have not been proposed. Recently, dynamic models of entire MGs based on droop and free-droop control structures have been proposed [34,45]. These models propose CPES models that consider communication topologies, the controller interactions and the distribution network constraints. Although these approaches integrate a dynamic model of the controllers, these do not consider the dynamic effects of inverter physical components like filter capacitors and inductance and dynamic components in the loads.

3.2. Cybernetic Requirements and Challenges in the New MG Power Sharing Control Strategies

3.2.1. Communication Architectures

Three main communication architectures used for the communication-based power sharing control strategies have been identified, namely [10]:

1.　Centralized: Communications between each IDG with an Energy Management System (EMS) (Some previous literature calls to the EMS also as Microgrid Central Controller (MGCC) [51]).
2.　Distributed: Communication links among neighbor DGs.
3.　Hybrid: Using centralized and distributed architectures together.

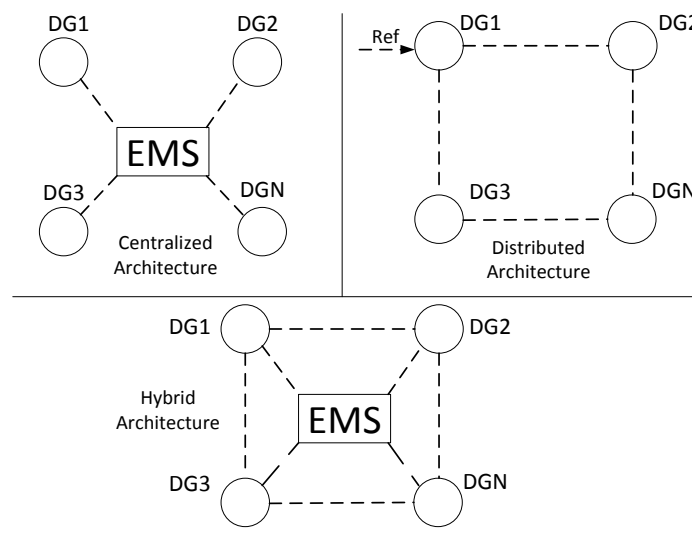The communication architectures for power sharing control in IMG are illustrated in Figure 4.

Figure 4. Communication architectures for power sharing control [10].

3.2.2. Communication Requirements

The characteristics of the communication network are an important cybernetic component to evaluate the operation performance of an MG [28]. The information of voltage and frequency values between DG local controllers as well as power measurements is typical information that is required to share using communication infrastructure in most of the secondary control strategies [25,45,52]. On the other hand, cybernetic signals such as incremental costs and energy prices could be required to the tertiary level of control.

Recent works have proposed the link failure and sampling period test as relevant characteristics of the communication infrastructure that should be evaluated on the performance of an MG control technique [45,52]. Thereby, communication latency is a constraint for the control strategies that require communication infrastructure [53]. This characteristic have been also defined as low bandwidth communication network requirement for secondary and tertiary controllers [45,52]. Additionally, the data dropout or pocket losses are performance parameters that have been analyzed for some secondary control strategies [54], whose values of 50% and 95% of pocket losses have been used for the performance test under 100ms of communication time delays.

3.2.3. Communication Time Delays and Package Losses

The impact of time delays in the different information flows on the control levels is one of the most significant challenges that the new control strategies in MGs need to include in the modeling and

design process. These impacts on the hierachical MG control levels have been studied by different authors, including primary level [26], secondary level [27], and tertiary level [28]. The main impact of the time delays on the feedback and control signals is identified under the stability performance. For this reason, establishing the potential vulnerabilities of each control strategy to communication time delays is a main characteristic that a cyber-physical model should include.

3.2.4. Cyber Security

An important concern about the operation of an MG is the vulnerability under a potential cyber attacks. In this way, recent literature has highlighted the importance of developing new tools to prevent random failures and deliberated attacks, which could lead to detrimental effects on the system [21]. Among the safety events that should be considered in the MG operation, we have [24]:

- False-data injection attack (FDIA),
- Denial of service,
- Jamming,
- Random attacks.

Only some works on prevention strategies for cyber attacks in MGs have been proposed [24], and the standardization of this methodologies as well as the development of adequate cyber-physical models are open to further research. Overall, a proper dynamic modelling for an MG that considers cyber physical properties, including dynamics loads, network constraints and communication topologies and which offers an adequate flexibility to zooming out and zooming in is likely to be an open challenge in this area. In the next section, CPES modules are proposed by the different approaches to cope with the power sharing issues. The developed CPES modules allow the designer to identify the controller signals and components that eventually require a time delay analysis process, communication requirements evaluation, and cyber-attack prevention strategies.

4. Cyber Physical Energy System Modules for Power Sharing Controllers

In this section, different CPES modules are developed for each power sharing strategy. Each module characterizes local sensing and actuation as well as physical and cybernetic input and output signals, and internal dynamics.

4.1. Adaptive Voltage Droop Control

The adaptive voltage droop control strategy is proposed based on the conventional droop controller, and using centralized communication with a central energy management system (EMS) achieves accurate power sharing [42]. Additionally, robustness to eventual communication interruptions and delays have been tested. The local output reactive power ($q_{m,i}$) of each IDG is sent to the EMS, which calculates the reactive power references (q_i^*), based on the nominal power of each IDG and the demanded total load. In this way, each IDG tunes the variable $\tilde{n}$ using a integral action under the reactive power error as it is shown in the following equation:

$$\tilde{n} = k_i \int_0^t (q_{m,i} - q_i^*), \tag{14}$$

where $v_i = v_n - (n + \tilde{n})q_{m,i}$. The adaptive droop control CPES module is shown in Figure 5. It can be seen that this strategy requires only one external cybernetic signal input and output (q_i^* and $q_{m,i}$, respectively). These signals are sent and received from and to the EMS. The authors in [42] claim that this approach uses low bandwidth communication links and is non-vulnerable to communication failure and communication delays. However, these cyber-physical characteristics have not been demonstrated rigorously, and the requirement of centralized communication could affect the reliability

in case of single point failures. A similar secondary controller was proposed to adjust the reference voltage (v_i) based on a proportional-integral actions given by [54]:

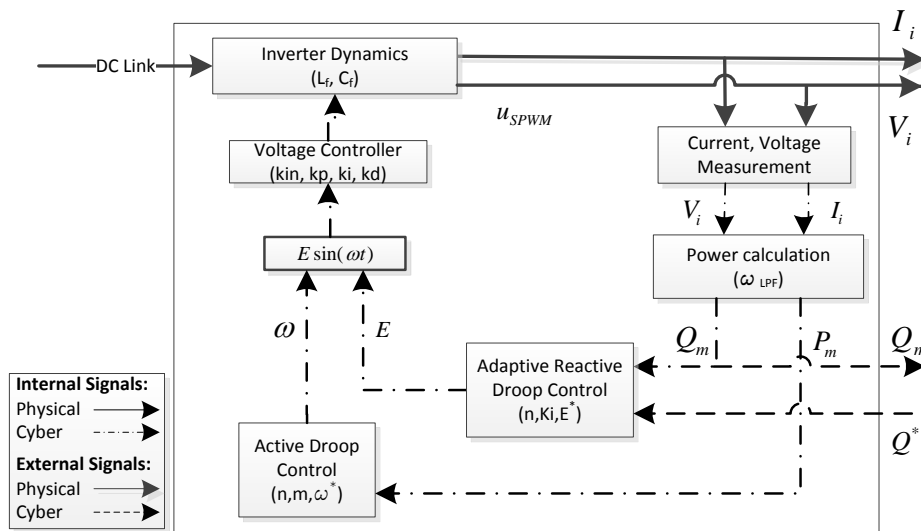$$\tilde{n} = k_p(q_{m,i} - q_i^*) + k_i \int_0^t (q_{m,i} - q_i^*).$$

(15)

Figure 5. IDG CPES module (adaptive droop control).

4.2. Consensus Based Approach

A consensus-based distributed voltage control to deal with the power sharing problem was proposed in [34]. This strategy uses sparse communications among inverters without central communications. The authors provide necessary and sufficient conditions for local exponential stability. Applying the CPES modeling methodology, a CPES module for this strategy is developed and shown in Figure 6. The distributed voltage controller is proposed as:

$$v_i = v_n - k_i \int_0^t e_i(\tau) d\tau,$$

(16)

where

$$e_i(\tau) = \sum_{k \sim C_i} \left(\frac{q_i^m}{\chi_i} - \frac{q_k^m}{\chi_k} \right),$$

(17)

where χ_i, and χ_k are the weighting factors according to the proportional power sharing Definition 1, and k_i is a control gain. The power calculation model as well as the frequency droop controller model are the same as the conventional droop control strategy. The model does not include dynamic components of the low level inner controls, inverter filters and dynamic loads. Neglecting these characteristics could affect the model accuracy and the general reliability of the MG control design [50].
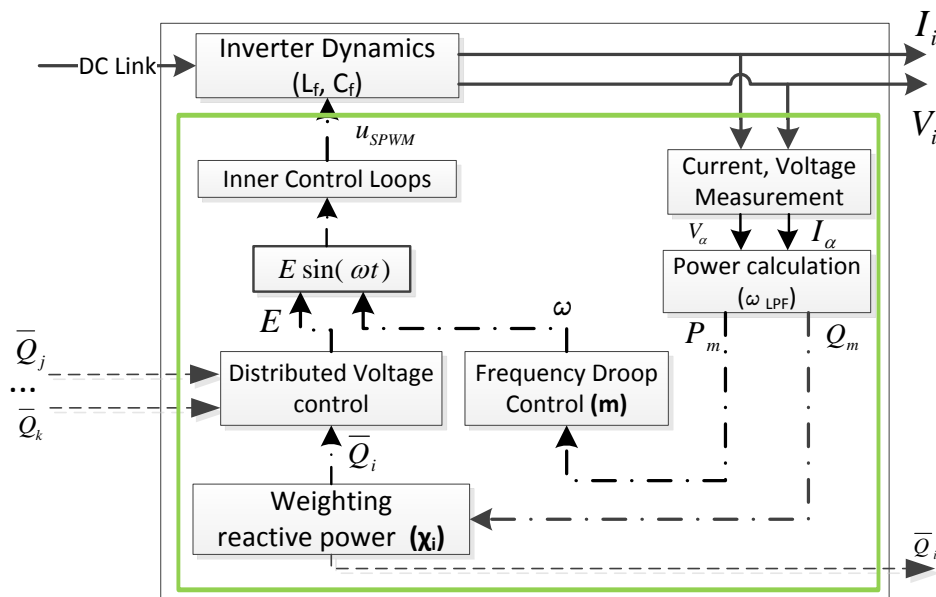
Figure 6. IDG CPES module (consensus protocol approach).

4.3. Cooperative Droop Free Secondary Control

A cooperative droop-free secondary controller was proposed in [45]. This strategy uses neighbor communications and a limited centralized communication, defined as a hybrid communication architecture (see Figure 4). A CPES IDG module for this approach is shown in Figure 7. As we can see, three main blocks perform the power sharing control action: voltage estimator and regulator, reactive power regulator, and the active power regulator. The voltage estimator and regulator adjust the set point voltage magnitude (v_i) by two correction terms, δv_i^1 and δv_i^2, where:

$$v_i = v_n + \delta v_i^1 + \delta v_i^2 \tag{18}$$

and δv_i^1 is the output of an Proportional-Integral (PI) action under the error signal produced by the comparison between the rated voltage (v_n) and the estimated average voltage $\overline{v}_i$. The voltage estimator is implemented based on a dynamic consensus protocol as [45]:

$$\overline{v_i} = v_i + \int_0^t \sum_{j \in C_i} \left(\overline{v}_j - \overline{v}_i \right), \tag{19}$$

where $\overline{v}_j$ and $\overline{v}_i$ are the average estimated voltage in the *ith* and *jth* node, respectively. On the other hand, the reactive power regulator produces a second voltage correction term (δv_i^2), which is adjusted trough the neighborhood reactive loading mismatch mq_i, given by:

$$mq_i = \sum_{j \in N_i} ba_{ij} \left(q_j^{norm} - q_i^{norm} \right), \tag{20}$$

where b is a control parameter, a_{ij} is an element of the adjacency matrix obtained from the communication graph and q_j^{norm} and q_i^{norm} are the normalized measured reactive power from the IDG_i and their neighbours IDG_j. Finally, the active power regulator computes the frequency correction factor $\delta \omega_i$, where the loading mismatch is given by $\delta \omega_i = \sum_{j \in N_i} ca_{ij} \left(p_j^{norm} - p_i^{norm} \right)$, where p_j^{norm} and

p_i^{norm} are the normalized output reactive power from the IDG_i and their neighbors IDG_j, and c is a control parameter.

The CPES module of the cooperative-free droop secondary control strategy is presented in Figure 7. From the module, we can see that this strategy requires both centralized communication with the EMS in order to obtain the cybernetic signals v_n and ω_n, and communications between IDG neighbors to obtain the cybernetic signals of $\overline{v_j}$, v_j^{norm} and p_j^{norm}. A similar decentralized approach based on the consensus theory can be found in [55], where a small signal stability analysis is presented and communication failure resiliency is analyzed based on experimental study cases.
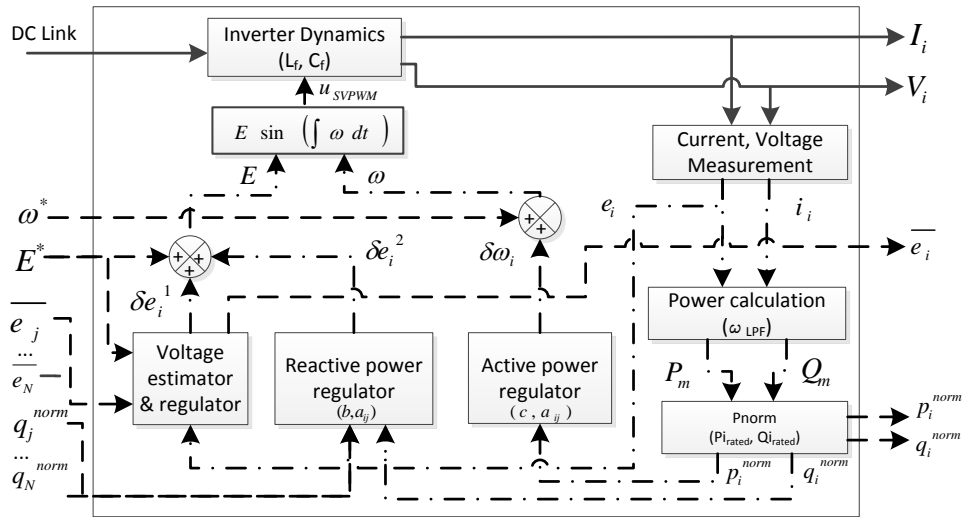

Figure 7. IDG CPES module (cooperative free-droop approach).

4.4. Adaptive Virtual Impedance

A power sharing control strategy using virtual components was proposed in [47]. A CPES module for this control strategy was developed as is shown in Figure 8. This approach modifies the conventional virtual impedance method, which emulates a dominant virtual output impedance to reduce the effect of feeder impedance mismatch. Hence, two additional droops (δV_d and δV_q) are introduced on the voltage droop references (v_d^* and v_q^*) in a d−q reference as:

$$v_{d,i} = v_{d,n} - (k_v \cdot i_{d,i} + k_v \cdot i_{q,i}), \tag{21}$$

$$v_{q,i} = v_{q,n} - (k_v \cdot i_{d,i} - k_v \cdot i_{q,i}), \tag{22}$$

where i_d and i_q are the measured output currents in d-q frame and k_v is the virtual impedance parameter (it can be noted that in this approach the virtual resistance (r_v) is assumed to be equal to the virtual reactance (x_v), it is $k_v = r_v = r_v$). Finally, an integral action adjusts adaptively the virtual impedance parameter k_v as follows:

$$k_v = k_i \int_0^t (q_i^* - q_{m,i}). \tag{23}$$

Similarly to the adaptive voltage droop control approach, this method uses a centralized communication architecture, where the virtual impedance parameter is determined by a cybernetic signal (q^*) sent from the EMS and the reactive power measured (q_m) is sent to the EMS.
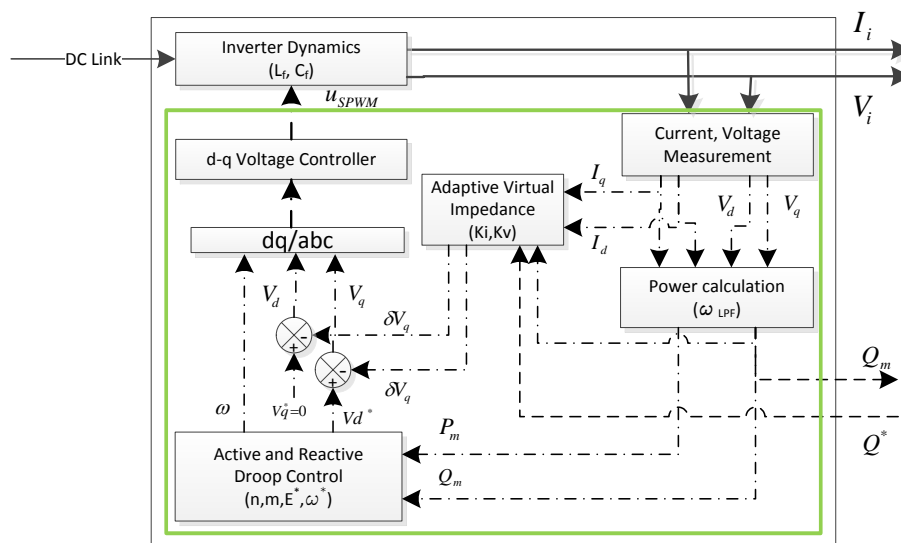
Figure 8. IDG CPES module (adaptive virtual impedance).

Using this approach, an accurate reactive power sharing is achieved and, in case of possible communication faults after the tuning process of the parameter k_v, the errors are reduced to lower values than the conventional approaches (virtual impedance and droop control). Likewise, the authors in [47] claim that this approach is insensitive to communications time delays. However, an inadequate design of the virtual impedance values (r_v and x_v) could affect the system stability and the dynamics performance [17,18]; additionally, the robustness to time delays and communication faults have not been rigorously analyzed. This approach is extended in [56] where a distributed consensus protocol is developed to adaptively tune the virtual impedance of the local primary controllers at the fundamental frequency and selected harmonic frequencies, and achieve accurate reactive, harmonic and imbalance power sharing.

4.5. Synchronous-Reference-Frame Virtual Impedance

A new decentralized power sharing control strategy that does not require power calculations was proposed in [57]. A CPES module of this approach is presented in Figure 9. This control strategy implements a resistive virtual impedance to control the reactive and active power flow based on the $i_q - \omega$ and $i_d - V$ droop characteristics. Thus, the output current relationships of each inverter can be generalized for n IDGs as:

$$i_{d,1} \cdot r_{vd,1} = i_{d,2} \cdot r_{vd,2} = ... = i_{d,n} \cdot r_{vd,n}, \tag{24}$$

$$i_{q,1} \cdot r_{vq,1} = i_{q,2} \cdot r_{vq,2} = ... = i_{q,n} \cdot r_{vq,n}, \tag{25}$$

where $r_{vd,i}$ and $r_{vq,i}$ ($i = 1, 2, ..., n$), are the resistance virtual output impedance in d and q reference frame, respectively.
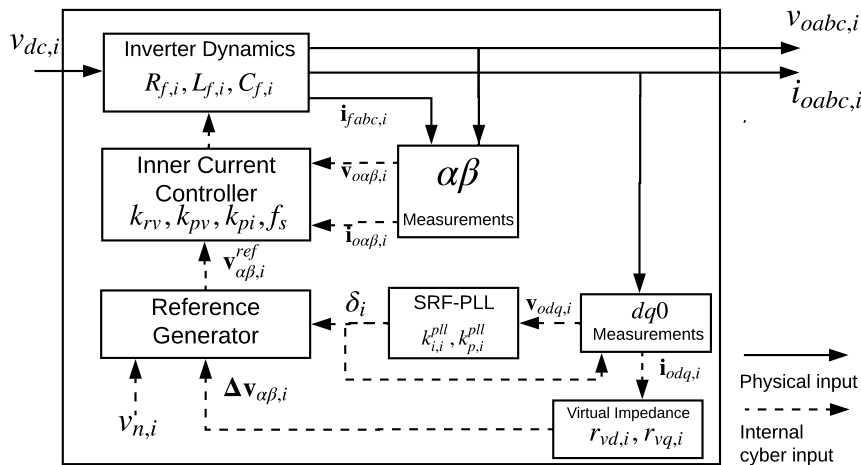
Figure 9. IDG CPES module (SRF virtual impedance loop).

Considering the relationship introduced above, the active and reactive power output may be accurately shared as:

$$p_1 \cdot r_{vd,1} = p_2 \cdot r_{vd,2} = ... = p_n \cdot r_{vd,n}, \tag{26}$$

$$q_1 \cdot r_{vq,1} = q_2 \cdot r_{vq,2} = ... = q_n \cdot r_{vq,n}. \tag{27}$$

The main benefits of using local information-based strategies are better reliability, plug and play functionality and lower implementation cost [58]. Additionally, it is important to note that the assumption of a dominant resistive inverter output limits the scope of this strategy in terms of maximum inductive and resistive line impedance [57]. On the other hand, the use of local signals (d−q output currents ($i_{d,i}$ and $i_{q,i}$)) leads to not needing local power calculation methods and faster response with respect to methods based on power calculation including conventional methods and most of the new strategies [10].

4.6. Cooperative-Adaptive SRF Virtual Impedance Algorithm

In a previous work [25], it has been shown that the Synchronous-Reference-Frame Virtual Impedance strategy does not achieve accurate proportional power sharing in a mismatched line impedance scenario. Additionally, it shows that accurate proportional power sharing performance can be achieved with a proper online tuning of the parameters $r_{vd,i}$ and $r_{vq,i}$. In order to tune the parameters without an accurate knowledge of the line parameters (i.e., $r_{l,i}$ and $l_{l,i}$), an online adaptive algorithm is proposed. The adaptive algorithm to tune the virtual resistance parameters is given by [25]:

$$r_{vd,i} = r_{vd}^* + k_i \int_0^t e_{d,i}(\tau)d\tau,$$
$$e_{d,i}(\tau) = \sum_{k \sim C_i} \left(\frac{i_{od,i}}{\gamma_i} - \frac{i_{od,k}}{\gamma_k} \right), \tag{28}$$

$$r_{vqi} = r_{vq}^* + k_i \int_0^t e_{qi}(\tau)d\tau,$$
$$e_{q,i}(\tau) = \sum_{k \sim C_i} \left(\frac{i_{oq,i}}{\chi_i} - \frac{i_{oq,k}}{\chi_k} \right), \tag{29}$$

where $k_i \in \mathbb{R}_{\geq 0}$ is an integral controller parameter and $r_{vd}^* \in \mathbb{R}_{\geq 0}$ and $r_{vq}^* \in \mathbb{R}_{\geq 0}$ are the base virtual resistor parameters. A cyber-physical module of the Cooperative-Adaptive SRF Virtual Impedance strategy is shown in Figure 10. Note that this strategy only requires a distributed communication

network between neighbor IDGs to avoid the conventional requirement of centralized control and communications. In the module, the cybernetic external inputs are given by the column vector $\bar{\mathbf{i}}_{odq,C_i}$ given by:

$$\bar{\mathbf{i}}_{od,C_i} = \text{col}\left(\frac{i_{oq,i}}{\chi_i}\right) \in C_i, \tag{30}$$

$$\bar{\mathbf{i}}_{oq,C_i} = \text{col}\left(\frac{i_{oq,i}}{\gamma_i}\right) \in C_i. \tag{31}$$
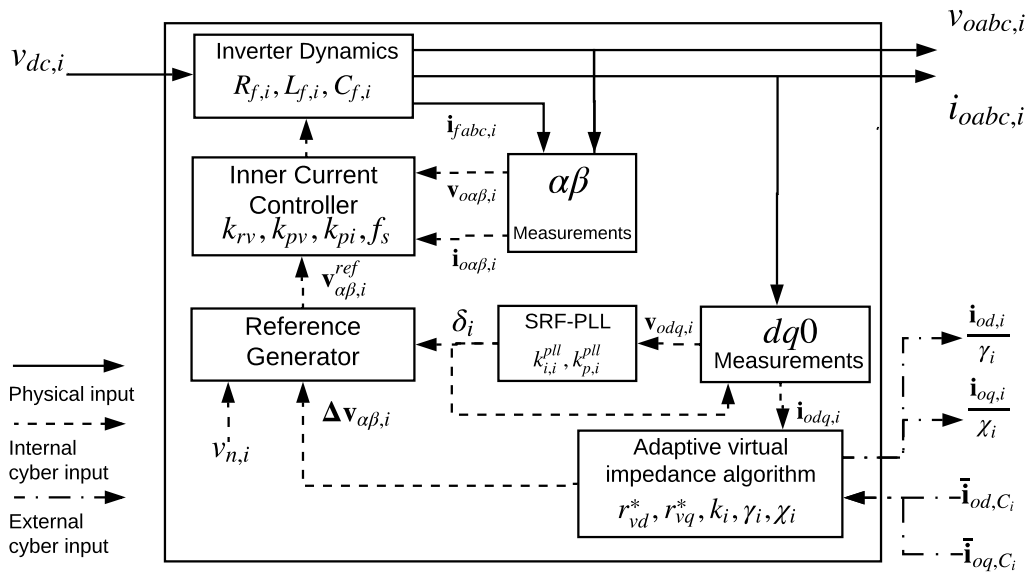
Figure 10. IDG CPES module (Cooperative-Adaptive SRF virtual impedance algorithm).

The CPES module allows for analyzing in a systematic manner possible communication time delays on the control signals, which could affect the performance and stability of MG. Preliminary simulation results have shown the potential impact of the constant communication delays on the distributed communication channels [25]. As a conclusion, it has been found that time delays on the communication channels could affect the power sharing performance and high time delays eventually could lead to instability of the system. However, in a small two IDGs case, the obtained time delay margin is consistent with the available communication technology and typical communication latency requirements [25]. A generalization of these results, integrating the CPES module developed in this paper, is an area for further research.

5. Discussion

In this section, a requirements analysis and comparison of the power sharing control strategies presented in the previous section is performed. Firstly, a summary of the main cybernetic requirements that have been tested on each strategy are summarized in Table 1. These requirements include communication time delays and bandwidth, data dropout (or package losses), communication architecture, and communication failure test. Additionally, a comparison of the number of cybernetic outputs and outputs based on the CPES modules developed in the previous section is included, where *k* denotes the number of neighbors of an IDG. This information can be used as a complexity and communication cost index (owing to the number of external cybernetic signals are proportional to the information channels required). In a similar way, we can see that although the centralized communication architecture requires less cybernetic outputs and inputs, it requires a higher number of

communication links and could be more vulnerable to single point failure events. The typical values for the time delay analysis vary between 1 ms and 2 s. The bandwidth test has only been tested on the cooperative-free droop strategy using a range between 1 kHz and 100 kHz. In a similar way, the data dropout test has only been performed on the adaptive voltage droop control strategy, using values of 50% and 95% of package losses. Finally, the communications failure test has been performed on a single point scheme, and any strategy has been tested with multiple point failure schemes. As it can be seen, there is not a consensus in the literature about the type of cybernetic parameters that should been evaluated and what standard values should be used in the tests. This summary can be a useful contribution towards the standardization of the cyber-physical performance tests for MG operation.

In addition, a comparison of the different control strategies is presented in Table 2 that includes the advantages and disadvantages of the different proposals. Strategies based on communication achieve a precise exchange of power, solving the main drawback of conventional approaches. On the other hand, information-based local strategies are still interesting due to their faster response and plug-and-play capabilities, where the synchronous frame of reference virtual impedance strategy can improve the stability performance and the transient response. It is interesting to note that any power sharing control strategy has included cyber-security considerations in a systematic scheme, despite the important concerns that this area has recently generated and that were presented in Section 3.2.4.

Table 1. Cybernetic requirements analysis.

Control Strategy	Communication Time Delays	Communication Bandwidth	Data Dropout	Communication Architecture (See Figure 4)	Communication Failure	CPES Module (Cyber Inputs-Outputs)
Adaptive Voltage Droop Control [42,54]	200 ms, 1 s, 2 s	Not tested	50%, 95%	Centralized	Single point	Figure 5 (1−1)
Consensus Based Approach [34]	Not tested	Not tested	Not tested	Distributed	Not tested	Figure 6 (k−1)
Cooperative Droop Free [45,55]	1 ms, 50 ms, 150 ms	100 kHz, 10 kHz, 1 kHz	Not tested	Hybrid	Single point	Figure 7 (3 + 2k)
Adaptive Virtual Impedance [47]	0.1, 0.05 s	Not tested	Not tested	Centralized	Single point	Figure 8 (1−1)
SRF Virtual Impedance [57,59]	Not required	Not required	Not required	Not required	Not required	Figure 9 (0−0)
Cooperative-Adaptive SRF-VI [25]	0.1 s 0.3 s	Not tested	Not tested	Distributed	Not tested	Figure 10 (2k−2)

Table 2. Power sharing control strategies summary.

Category	Potential Advantages	Potential Disadvantages	References
Conventional Droop Control	Accurate active power sharing Use of local information	Reactive power sharing error Voltage and frequency recovery requirement Slow response and Stability performance	[60–63]
Adaptive Voltage Droop Control	Accurate active and reactive power sharing	Higher communication cost Voltage and frequency recovery requirement	[42,54]
Adaptive Virtual Impedance	Accurate active and reactive power sharing	Line impedance independence	[47]
Consensus Based Approach	Accurate power sharing Impedance parameters independence Lower communication cost	Voltage and Frequency Recovery Communication faults and delays robustness analysis not available	[34]
Cooperative Droop Free	Accurate power sharing Voltage and frequency regulation	Distributed Communications required	[45,55]
SRF Virtual Impedance	Use of local information Free active/reactive power calculation Faster response	Requirement of voltage recovery Line impedance restrictions SRF-PLL based synchronization required	[57,59]
Cooperative-Adaptive SRF-VI	Accurate active and reactive power sharing Free power calculation	Requirement of voltage recovery SRF-PLL based synchronization required	[25]

6. Conclusions

In this work, recent power sharing control strategies for MGs has been analyzed using a cyber-physical modeling methodology. These new control strategies use cybernetic components including virtual components and communication infrastructure. In this context, a cyber-physical modeling approach has been applied to build integrated CPES modules of each control approach, and two main control categories have been identified as: communication-based strategies and local information-based strategies. Cybernetic characteristics and parameters have been identified for the power sharing control techniques, including three main communication architectures, and typical time delay, bandwidth and data dropout testing values. There is not a consensus in the literature about the type of cybernetic parameters that should been evaluated and what standard values should be used in the tests. The results presented in Section 5 can be a contribution towards the standardization of the cyber-physical performance tests for the MG operation. A standardized cyber-physical modeling and control strategy for power sharing seems to be an open challenge in the MGs area; this control strategy is likely to include cybernetic components such as communication and computational requirements, and robustness to cybernetic constraints such as communication time delays.

Author Contributions: Conceptualization, Methodology, Software, Validation and Formal Analysis, C.A.M. Investigation, C.A.M. and A.F.A.; Resources H.R.P., J.C.V., and J.M.G.; Writing—Original Draft Preparation, C.A.M.; Writing—Review and Editing, C.A.M. and A.F.A.; Visualization, C.A.M.; Supervision, H.R.P., J.C.V. and J.M.G.; Project Administration, H.R.P.; Funding Acquisition, H.R.P., J.C.V. and J.M.G.

Conflicts of Interest: The authors declare no conflict of interest. The founding sponsors had no role in the design of the study; in the collection, analyses, or interpretation of data; in the writing of the manuscript, and in the decision to publish the results

References

1. Wang, Z.; Wu, W.; Zhang, B. A Distributed Control Method With Minimum Generation Cost for DC Microgrids. *IEEE Trans. Energy Convers.* **2016**, *31*, 1462–1470. [CrossRef]
2. Lasseter, R. Smart Distribution: Coupled Microgrids. *Proc. IEEE* **2011**, *99*, 1074–1082. [CrossRef]
3. Peng, F.Z.; Li, Y.W.; Tolbert, L.M. Control and protection of power electronics interfaced distributed generation systems in a customer-driven microgrid. In Proceedings of the 2009 IEEE Power Energy Society General Meeting, Calgary, AB, Canada, 26–30 July 2009; pp. 1–8. [CrossRef]
4. Bevrani, H.; Watanabe, M.; Mitani, Y. Microgrid Control: Concepts and Classification. In *Power System Monitoring and Control*; Wiley-IEEE Press: Hoboken, NJ, USA, 2014; p. 288. [CrossRef]
5. Mahmud, M.; Hossain, M.; Pota, H.; Oo, A. Robust Nonlinear Distributed Controller Design for Active and Reactive Power Sharing in Islanded Microgrids. *IEEE Trans. Energy Convers.* **2014**, *29*, 893–903. [CrossRef]
6. Zamora, R.; Srivastava, A.K. Controls for microgrids with storage: Review, challenges, and research needs. *Renew. Sustain. Energy Rev.* **2010**, *14*, 2009–2018. [CrossRef]
7. Han, H.; Hou, X.; Yang, J.; Wu, J.; Su, M.; Guerrero, J.M. Review of Power Sharing Control Strategies for Islanding Operation of AC Microgrids. *IEEE Trans. Smart Grid* **2016**, *7*, 200–215. [CrossRef]
8. Vandoorn, T.; De Kooning, J.; Meersman, B.; Vandevelde, L. Review of primary control strategies for islanded microgrids with power-electronic interfaces. *Renew. Sustain. Energy Rev.* **2013**, *19*, 613–628. [CrossRef]
9. Lopes, J.A.P.; Moreira, C.L.; Madureira, A.G. Defining control strategies for MicroGrids islanded operation. *IEEE Trans. Power Syst.* **2006**, *21*, 916–924. [CrossRef]
10. Macana, C.A.; Pota, H. New trends of reactive power sharing control for islanded microgrids: A cyber-physical review. In Proceedings of the 2016 IEEE Innovative Smart Grid Technologies–Asia (ISGT-Asia), Melbourne, VIC, Australia, 28 November–1 December 2016; pp. 353–358. [CrossRef]
11. Chandorkar, M.; Divan, D.; Adapa, R. Control of parallel connected inverters in standalone AC supply systems. *IEEE Trans. Ind. Appl.* **1993**, *29*, 136–143. [CrossRef]

12. Tuladhar, A.; Jin, H.; Unger, T.; Mauch, K. Control of parallel inverters in distributed AC power systems with consideration of line impedance effect. *IEEE Trans. Ind. Appl.* **2000**, *36*, 131–138. [CrossRef]

13. Guerrero, J.; Matas, J.; de Vicuna, L.G.; Castilla, M.; Miret, J. Decentralized Control for Parallel Operation of Distributed Generation Inverters Using Resistive Output Impedance. *IEEE Trans. Ind. Electron.* **2007**, *54*, 994–1004. [CrossRef]

14. Li, Y.; Li, Y.W. Power Management of Inverter Interfaced Autonomous Microgrid Based on Virtual Frequency-Voltage Frame. *IEEE Trans. Smart Grid* **2011**, *2*, 30–40. [CrossRef]

15. Zhong, Q.C. Robust Droop Controller for Accurate Proportional Load Sharing Among Inverters Operated in Parallel. *IEEE Trans. Ind. Electron.* **2013**, *60*, 1281–1290. [CrossRef]

16. Lee, C.T.; Chu, C.C.; Cheng, P.T. A New Droop Control Method for the Autonomous Operation of Distributed Energy Resource Interface Converters. *IEEE Trans. Power Electron.* **2013**, *28*, 1980–1993. [CrossRef]

17. Matas, J.; Castilla, M.; de Vicuña, L.; Miret, J.; Vasquez, J. Virtual Impedance Loop for Droop-Controlled Single-Phase Parallel Inverters Using a Second-Order General-Integrator Scheme. *IEEE Trans. Power Electron.* **2010**, *25*, 2993–3002. [CrossRef]

18. He, J.; Li, Y.W. Analysis, Design, and Implementation of Virtual Impedance for Power Electronics Interfaced Distributed Generation. *IEEE Trans. Ind. Appl.* **2011**, *47*, 2525–2538. [CrossRef]

19. Kim, J.; Guerrero, J.; Rodriguez, P.; Teodorescu, R.; Nam, K. Mode Adaptive Droop Control With Virtual Output Impedances for an Inverter-Based Flexible AC Microgrid. *IEEE Trans. Power Electron.* **2011**, *26*, 689–701. [CrossRef]

20. Planas, E.; de Muro, A.G.; Andreu, J.; Kortabarria, I.; de Alegría, I.M. General aspects, hierarchical controls and droop methods in microgrids: A review. *Renew. Sustain. Energy Rev.* **2013**, *17*, 147–159. [CrossRef]

21. Yu, X.; Xue, Y. Smart Grids: A Cyber–Physical Systems Perspective. *Proc. IEEE* **2016**, *104*, 1058–1070. [CrossRef]

22. Macana, C.; Quijano, N.; Mojica-Nava, E. A survey on Cyber Physical Energy Systems and their applications on smart grids. In Proceedings of the 2011 IEEE Pes Conference on Innovative Smart Grid Technologies Latin America (Isgt la), Medellin, Colombia, 19–21 October 2011; pp. 1–7. [CrossRef]

23. Wang, C.; Zhang, T.; Luo, F.; Li, F.; Liu, Y. Impacts of Cyber System on Microgrid Operational Reliability. *IEEE Trans. Smart Grid* **2018**. [CrossRef]

24. Beg, O.A.; Johnson, T.T.; Davoudi, A. Detection of False-Data Injection Attacks in Cyber-Physical DC Microgrids. *IEEE Trans. Ind. Inf.* **2017**, *13*, 2693–2703. [CrossRef]

25. Macana, C.A.; Pota, H.R. Adaptive synchronous reference frame virtual impedance controller for accurate power sharing in islanded ac-microgrids: A faster alternative to the conventional droop control. In Proceedings of the 2017 IEEE Energy Conversion Congress and Exposition (ECCE), Cincinnati, OH, USA, 1–5 October 2017; pp. 3728–3735. [CrossRef]

26. Liu, J.; Miura, Y.; Ise, T. Comparison of Dynamic Characteristics Between Virtual Synchronous Generator and Droop Control in Inverter-Based Distributed Generators. *IEEE Trans. Power Electron.* **2016**, *31*, 3600–3611. [CrossRef]

27. Coelho, E.A.A.; Wu, D.; Guerrero, J.M.; Vasquez, J.C.; Dragičević, T.; Stefanović, C.; Popovski, P. Small-Signal Analysis of the Microgrid Secondary Control Considering a Communication Time Delay. *IEEE Trans. Ind. Electron.* **2016**, *63*, 6257–6269. [CrossRef]

28. Khalil, A.; Rajab, Z.; Alfergani, A.; Mohamed, O. The impact of the time delay on the load frequency control system in microgrid with plug-in-electric vehicles. *Sustain. Cities Soc.* **2017**, *35*, 365–377. [CrossRef]

29. Li, H.; Zang, C.; Zeng, P.; Yu, H.; Li, Z. A stochastic programming strategy in microgrid cyber physical energy system for energy optimal operation. *IEEE/CAA J. Autom. Sin.* **2015**, *2*, 296–303. [CrossRef]

30. Ban, M.; Shahidehpour, M.; Yu, J.; Li, Z. A Cyber-Physical Energy Management System and Optimal Sizing of Networked Nanogrids with Battery Swapping Stations. *IEEE Trans. Sustain. Energy* **2018**. [CrossRef]

31. Ilic, M.; Xie, L.; Khan, U.; Moura, J. Modeling of Future Cyber Physical Energy Systems for Distributed Sensing and Control. *Trans. Syst. Man Cybern. Part A Syst. Hum. IEEE* **2010**, *40*, 825–838. [CrossRef]

32. Krause, P.C.; Wasynczuk, O.; Sudhoff, S.D.; Pekarek, S. *Analysis of Electric Machinery and Drive Systems*; John Wiley & Sons: Hoboken, NJ, USA, 2013.

33. IEEE. *IEEE Guide for Design, Operation, and Integration of Distributed Resource Island Systems with Electric Power Systems*; IEEE Std 1547.4-2011; IEEE: Hoboken, NJ, USA, 2011; pp. 1–54. [CrossRef]

34. Schiffer, J.; Seel, T.; Raisch, J.; Sezi, T. Voltage Stability and Reactive Power Sharing in Inverter-Based Microgrids with Consensus-Based Distributed Voltage Control. *IEEE Trans. Control Syst. Technol.* **2016**, *24*, 96–109. [CrossRef]

35. Pota, H. Droop control for islanded microgrids. In Proceedings of the 2013 IEEE Power & Energy Society General Meeting, Vancouver, BC, Canada, 21–25 July 2013; pp. 1–4. [CrossRef]

36. Yang, Y.; Blaabjerg, F. A new power calculation method for single-phase grid-connected systems. In Proceedings of the 2013 IEEE International Symposium on Industrial Electronics, Taipei, Taiwan, 28–31 May 2013; pp. 1–6. [CrossRef]

37. He, J.; Li, Y.W.; Guerrero, J.; Blaabjerg, F.; Vasquez, J. An Islanding Microgrid Power Sharing Approach Using Enhanced Virtual Impedance Control Scheme. *IEEE Trans. Power Electron.* **2013**, *28*, 5272–5282. [CrossRef]

38. Guerrero, J.; Garcia De Vicuna, L.; Matas, J.; Castilla, M.; Miret, J. Output Impedance Design of Parallel-Connected UPS Inverters With Wireless Load-Sharing Control. *IEEE Trans Ind. Electron.* **2005**, *52*, 1126–1135. [CrossRef]

39. Guerrero, J.; Garcia De Vicuna, L.; Matas, J.; Castilla, M.; Miret, J. A wireless controller to enhance dynamic performance of parallel inverters in distributed generation systems. *IEEE Trans. Power Electron.* **2004**, *19*, 1205–1213. [CrossRef]

40. Schiffer, J.; Zonetti, D.; Ortega, R.; Stankovic, A.M.; Sezi, T.; Raisch, J. Modeling of microgrids—From fundamental physics to phasors and voltage sources. *CoRR* **2015**, *28*, 51–67. [CrossRef]

41. Han, H.; Liu, Y.; Sun, Y.; Su, M.; Guerrero, J. An Improved Droop Control Strategy for Reactive Power Sharing in Islanded Microgrid. *IEEE Trans. Power Electron.* **2015**, *30*, 3133–3141. [CrossRef]

42. Mahmood, H.; Michaelson, D.; Jiang, J. Reactive Power Sharing in Islanded Microgrids Using Adaptive Voltage Droop Control. *IEEE Trans. Smart Grid* **2015**, *6*, 3052–3060. [CrossRef]

43. Milczarek, A.; Malinowski, M.; Guerrero, J. Reactive Power Management in Islanded Microgrid. Proportional Power Sharing in Hierarchical Droop Control. *IEEE Trans. Smart Grid* **2015**, *6*, 1631–1638. [CrossRef]

44. Macana, C.; Mojica-Nava, E.; Quijano, N. Time-delay effect on load frequency control for microgrids. In Proceedings of the 2013 10th IEEE International Conference on Networking, Sensing and Control (Icnsc), Evry, France, 10–12 April 2013; pp. 544–549. [CrossRef]

45. Nasirian, V.; Shafiee, Q.; Guerrero, J.; Lewis, F.; Davoudi, A. Droop-Free Distributed Control for AC Microgrids. *IEEE Trans. Power Electron.* **2016**, *31*, 1600–1617. [CrossRef]

46. Vaccaro, A.; Popov, M.; Villacci, D.; Terzija, V. An Integrated Framework for Smart Microgrids Modeling, Monitoring, Control, Communication, and Verification. *Proc. IEEE* **2011**, *99*, 119–132. [CrossRef]

47. Mahmood, H.; Michaelson, D.; Jiang, J. Accurate Reactive Power Sharing in an Islanded Microgrid Using Adaptive Virtual Impedances. *IEEE Trans. Power Electron.* **2015**, *30*, 1605–1617. [CrossRef]

48. Luo, L.; Dhople, S. Spatiotemporal Model Reduction of Inverter-Based Islanded Microgrids. *IEEE Trans. Energy Convers.* **2014**, *29*, 823–832. [CrossRef]

49. Rasheduzzaman, M.; Mueller, J.; Kimball, J. Reduced-Order Small-Signal Model of Microgrid Systems. *IEEE Trans. Sustain. Energy* **2015**, *6*, 1292–1305. [CrossRef]

50. Guo, X.; Lu, Z.; Wang, B.; Sun, X.; Wang, L.; Guerrero, J. Dynamic Phasors-Based Modeling and Stability Analysis of Droop-Controlled Inverters for Microgrid Applications. *IEEE Trans. Smart Grid* **2014**, *5*, 2980–2987. [CrossRef]

51. Kaur, A.; Kaushal, J.; Basak, P. A review on microgrid central controller. *Renew. Sustain. Energy Rev.* **2016**, *55*, 338–345. [CrossRef]

52. Lu, X.; Yu, X.; Lai, J.; Guerrero, J.M.; Zhou, H. Distributed Secondary Voltage and Frequency Control for Islanded Microgrids With Uncertain Communication Links. *IEEE Trans. Ind. Inf.* **2017**, *13*, 448–460. [CrossRef]

53. Gungor, V.C.; Sahin, D.; Kocak, T.; Ergut, S.; Buccella, C.; Cecati, C.; Hancke, G.P. A Survey on Smart Grid Potential Applications and Communication Requirements. *IEEE Trans. Ind. Inf.* **2013**, *9*, 28–42. [CrossRef]

54. Shafiee, Q.; Guerrero, J.M.; Vasquez, J.C. Distributed Secondary Control for Islanded Microgrids: A Novel Approach. *IEEE Trans. Power Electron.* **2014**, *29*, 1018–1031. [CrossRef]

55. Han, R.; Meng, L.; Ferrari-Trecate, G.; Coelho, E.A.A.; Vasquez, J.C.; Guerrero, J.M. Containment and Consensus-Based Distributed Coordination Control to Achieve Bounded Voltage and Precise Reactive Power Sharing in Islanded AC Microgrids. *IEEE Trans. Ind. Appl.* **2017**, *53*, 5187–5199. [CrossRef]

56.　Zhou, J.; Kim, S.; Zhang, H.; Sun, Q.; Han, R. Consensus-based Distributed Control for Accurate Reactive, Harmonic and Imbalance Power Sharing in Microgrids. *IEEE Trans. Smart Grid* **2017**, *9*, 2453–2467. [CrossRef]

57.　Guan, Y.; Guerrero, J.M.; Zhao, X.; Vasquez, J.C.; Guo, X. A New Way of Controlling Parallel-Connected Inverters by Using Synchronous-Reference-Frame Virtual Impedance Loop-Part I: Control Principle. *IEEE Trans. Power Electron.* **2016**, *31*, 4576–4593. [CrossRef]

58.　Olivares, D.; Mehrizi-Sani, A.; Etemadi, A.; Canizares, C.; Iravani, R.; Kazerani, M.; Hajimiragha, A.; Gomis-Bellmunt, O.; Saeedifard, M.; Palma-Behnke, R.; et al. Trends in Microgrid Control. *IEEE Trans. Smart Grid* **2014**, *5*, 1905–1919. [CrossRef]

59.　Guan, Y.; Meng, L.; Li, C.; Vasquez, J.; Guerrero, J. A Dynamic Consensus Algorithm to Adjust Virtual Impedance Loops for Discharge Rate Balancing of AC Microgrid Energy Storage Units. *IEEE Trans. Smart Grid* **2017**, *9*, 4847–4860. [CrossRef]

60.　Vasquez, J.C.; Guerrero, J.M.; Savaghebi, M.; Eloy-Garcia, J.; Teodorescu, R. Modeling, Analysis, and Design of Stationary-Reference-Frame Droop-Controlled Parallel Three-Phase Voltage Source Inverters. *IEEE Trans. Ind. Electron.* **2013**, *60*, 1271–1280. [CrossRef]

61.　Vasquez, J.C.; Guerrero, J.M.; Luna, A.; Rodriguez, P.; Teodorescu, R. Adaptive Droop Control Applied to Voltage-Source Inverters Operating in Grid-Connected and Islanded Modes. *IEEE Trans. Ind. Electron.* **2009**, *56*, 4088–4096. [CrossRef]

62.　Coelho, E.; Cortizo, P.; Garcia, P. Small-signal stability for parallel-connected inverters in stand-alone AC supply systems. *IEEE Trans. Ind. Appl.* **2002**, *38*, 533–542. [CrossRef]

63.　Mohamed, Y.R.; El-Saadany, E. Adaptive Decentralized Droop Controller to Preserve Power Sharing Stability of Paralleled Inverters in Distributed Generation Microgrids. *IEEE Trans. Power Electron.* **2008**, *23*, 2806–2816. [CrossRef]